Causes of Nonplanarity in Fluorinated 1,3?4?2,2,4-Benzodithiadiazines: Gas-Phase Electron Diffraction, Ab initio and DFT Structures

ARTICLE *in* BERICHTE DER DEUTSCHEN CHEMISCHEN GESELLSCHAFT · DECEMBER 2004

Impact Factor: 2.94 · DOI: 10.1002/ejic.200400601

Causes of Nonplanarity in Fluorinated 1,3λ⁴δ²,2,4-Benzodithiadiazines: Gas-Phase Electron Diffraction, Ab initio and DFT Structures

Andrew R. Turner,[a] Frank Blockhuys,[b] Christian Van Alsenoy,[b] Heather E. Robertson,[a] Sarah L. Hinchley,[a] Andrey V. Zibarev,[c] Alexander Yu. Makarov,[c] and David W. H. Rankin*[a]

Keywords: Antiaromaticity / Fluorinated 1,3λ⁴δ²,2,4-benzodithiadiazines / Molecular structure / Ab initio calculations / Density functional calculations

The gas-phase molecular structures of 6,8-difluoro-1,3λ⁴δ²,2,4-benzodithiadiazine and 5,6,7-trifluoro-1,3λ⁴δ²,2,4-benzodithiadiazine have been determined using quantum chemical calculations and electron diffraction via the SARACEN method of structural analysis. Of particular interest was the planarity or nonplanarity of the heterocyclic fragments of the molecules. It was shown that the difluoro compound is planar with respect to the heterocyclic fragment [folding angle: 0.0(5)° (figures in parenthesis indicate e.s.d.s in the final digits)] and that the trifluoro compound probably deviates from planarity to a small extent [folding angle: 4.0(–30;+3)°; the large uncertainty in the value of this angle is due to the low-frequency, large-amplitude vibrational motion associated with the folding of the heterocyclic fragment]. Pertinent structural parameters from the electron diffraction data (r_{h1} structure) of the difluoro compound are *av*[*r*(S=N)] = 155.7(7) pm, *r*(S–N) = 175.8(5) pm, *r*(C–S) = 176.6(8) pm and *r*(C–N) = 141.6(2) pm. For the trifluoro compound the equivalent structural parameters are *av*[*r*(S=N)] = 155.5(7) pm, *r*(S–N) = 170.7(6) pm, *r*(C–S) = 180.6(8) pm and *r*(C–N) = 140.6(2) pm. The gas-phase electron diffraction structures have been compared with results from ab initio and DFT calculations and also with experimental solid-state structures.

Introduction

Antiaromatic structures (i.e. those with 4*n* π-electrons) containing a benzenoid ring fused to a heterocyclic ring have been the subject of recent scrutiny due to their unusual structural properties.[1−4] Of particular interest have been 1,3λ⁴δ²,2,4-benzodithiadiazine and its fluorinated derivatives. The basic structural unit of these compounds consists of a benzene ring fused to a S_2N_2 fragment to give a 12 π-electron system. A gas-phase electron diffraction (GED) study of the parent compound 1,3λ⁴δ²,2,4-benzodithiadiazine (**1**)[3] showed that the heterocyclic fragment adopts a nonplanar conformation in the gas phase. In the same study it was shown that the tetrafluoro derivative (5,6,7,8-tetrafluoro-1,3λ⁴δ²,2,4-benzodithiadiazine, compound **2**) has a planar heterocyclic fragment in the gas phase. The nonplanar conformation of compound **1** was rationalised as a pseudo-Jahn−Teller distortion[5] which minimises the destabilisation caused by the antiaromaticity. For the tetrafluoro derivative it was postulated that a π-fluoro effect, due to the fluorine substituted in the 8-position, would counteract the pseudo-Jahn−Teller distortion leading to a planar conformation.

The study also revealed an unexpected conflict in the conformation predicted for compound **2** by ab initio molecular orbital (MO) methods and DFT calculations. The DFT calculations predicted the planar conformation as seen in the refined GED structure, whilst the MO calculations predicted the nonplanar conformation. This work extends the study by employing both GED and theoretical structural studies to deduce the gas-phase structures of the 6,8-difluoro derivative **3** and the 5,6,7-trifluoro derivative **4**. From the π-fluoro hypothesis we would expect compound **3** to show a planar conformation with respect to the heterocyclic fragment and compound **4** to show a nonplanar conformation. Along with **1** and **2**, these are the simplest accessible compounds that can be used to investigate the influence of fluorine substitution at position 8.

Preparation and Characterisation

Compounds **3** and **4** were prepared, purified and structurally characterised by single-crystal X-ray diffraction

[a] School of Chemistry, University of Edinburgh, West Mains Road, Edinburgh, EH9 3JJ, UK
Fax: (internat.) + 44-131-650-6452
E-mail: d.w.h.rankin@ed.ac.uk
[b] Department of Chemistry, University of Antwerp, Universiteitsplein 1, 2610 Wilrijk, Belgium
[c] Institute of Organic Chemistry, Russian Academy of Sciences, 630090 Novosibirsk, Russia
Supporting information for this article is available on the WWW under http://www.eurjic.org or from the author.

  DOI: 10.1002/ejic.200400601

studies as described in reference 4. IR spectra of the compounds in KBr were recorded on an FT Bruker Vector 22 spectrometer. Raman spectra were recorded with an FT Bruker IFS 66 spectrometer equipped with a Nd/YAG laser with an excitation line at 1064 nm.

GED Measurements

Electron diffraction data were captured with Kodak Electron Image photographic films using the Edinburgh gas-phase electron diffraction apparatus.[6] For compound **3**, at the short camera distance, the sample was maintained at a temperature of 423 K whilst the nozzle temperature was held at the higher temperature of 443 K to prevent sample condensation in the nozzle. At the long camera distance, the sample temperature was 381 K whilst the nozzle temperature was 413 K. The four corresponding temperatures for compound **4** were 431, 450, 386 and 413 K, respectively. The vapours were injected into the diffraction chamber through a metal nozzle with camera distances of approximately 98 mm and 250 mm. The electron accelerating voltage was approximately 40 kV, giving an electron wavelength close to 6 pm. The precise camera distances (d) and electron wavelengths (λ) were determined from scattering patterns for benzene vapour recorded immediately before or after the sample patterns. Details are given in Table 1, together with the weighting functions used to set up the diagonal elements of the weight matrix used in the least-squares refinement process (sw_1, sw_2), the s-ranges ($s_{min.}$, $s_{max.}$), the scale factors (k) and the correlation parameters (ratio of the off-diagonal terms to the diagonal terms of the weight matrix, q) which were used to define the immediate off-diagonal elements of the weight matrix.[7] The remaining elements of the weight matrix were set to zero.

Table 1. GED experimental details; figures in parentheses are the estimated standard deviations of the last digits

	d [mm]	Weighting functions [nm^{-1}]					q	k	λ [pm]
		Δs	$s_{min.}$	sw_1	sw_2	$s_{max.}$			
3	97.69	4	100	120	264	308	0.4406	0.673(15)	6.020
	256.19	2	20	40	128	150	0.3511	0.872(7)	6.020
4	97.85	4	100	120	264	308	0.4692	0.691(11)	6.020
	251.21	2	20	40	136	158	0.4009	0.861(7)	6.020

Details of the electron scattering patterns were converted into digital form using a PDS densitometer at the Institute of Astronomy in Cambridge. For compound **3**, the results spanning the ranges 20 nm^{-1} ≤ s ≤ 150 nm^{-1} and 100 nm^{-1} ≤ s ≤ 308 nm^{-1} and for compound **4**, the results spanning the ranges 20 nm^{-1} ≤ s ≤ 158 nm^{-1} and 100 nm^{-1} ≤ s ≤ 308 nm^{-1} were reduced and analysed using the ed@ed program[8] employing the scattering factors tabulated by Ross et al.[9]

Results and Discussion

Theoretical Studies

Calculations were performed at various levels, using the Gaussian98 suite of quantum chemistry programs,[10] to gauge the effects of different methodologies and basis sets on the structures. They also provide guidelines for the uncertainties of the SARACEN restraints[11] in the GED structure refinements (see GED Structure Refinements). The results are listed in Table 2 for compound **3** and in Table 3 for compound **4**.

The most obvious feature of the calculations is the disagreement between the ab initio results (MP2, 2nd order Møller-Plesset perturbation theory[12]) and the DFT results (B3LYP hybrid functional[13]) in the conformation predicted for compound **3**. The DFT calculations all agree on the planar conformation for the heterocyclic fragment while the ab initio calculations predict a nonplanar conformation. Although the two methods agree on the nonplanar conformation for compound **4**, the largest differences between the DFT and ab initio calculations are in the geometry of the heterocyclic fragment. The same patterns were noted and explained in a previous study of compounds of this type.[3] In short, the DFT results seem to agree consistently and more closely with previous GED experiments than the ab initio results.

GED Structure Refinements

6,8-Difluoro-1,3λ⁴δ²,2,4-benzodithiadiazine (3)

The refined structure and associated atom numbering scheme for compound **3** are shown in Figure 1. The molecular model was constructed in C_1 symmetry, thus allowing for the out-of-plane movement of the heterocyclic fragment. The $C_6H_2F_2$ fragment was assumed to be planar since all of the ab initio and DFT calculations show negligible deviations from planarity. Twenty-eight independent geometrical parameters were used to describe the molecular structure and these are defined in Table 4. Eleven of the parameters correspond to bond angles and four to torsional angles. The remaining thirteen describe the various bond lengths in the molecule. The two C−H distances are described by a single parameter (p_8) as are the two C−F distances (p_9). In both of these cases the calculations indicated insignificant differences between the two different occurrences of the bonds. The parameter p_1 corresponds to the mean of all the C−C and C−N bond lengths, with p_2 to p_7 corresponding to various combinations of differences between these distances. The mean and the difference between the S(12)−N(13) and S(12)−N(11) bond lengths are given by p_{12} and p_{13},respectively, since these distances are similar according to the ab initio and DFT calculations.

A force field in Cartesian coordinates, calculated using the DFT method with a B3LYP functional and a 6-311+G* basis set,[14] was used (after scaling, see below) to compute values for the root-mean-square (RMS) amplitudes of vibration (u_{h1}) and perpendicular distance corrections (k_{h1}) using the methods of Sipachev.[15] This takes account of the curvilinear motions of the atoms in the molecular vibrations and yields the r_{h1} structure from the refinement process.

IR and Raman spectra were recorded and used to scale the calculated force field to obtain the most realistic esti-

Table 2. Results of theoretical calculations for compound **3**; all distances in pm and all angles in degrees

Parameter	MP2 6-311+G*[a]	DFT-B3LYP 6-311+G*[a]	aug-cc-pVTZ[b]
r[C(1)−C(2)]	141.0	141.4	141.9
r[C(2)−C(3)]	139.5	138.2	137.4
r[C(3)−C(4)]	139.4	139.7	139.5
r[C(4)−C(5)]	139.0	137.7	137.4
r[C(5)−C(6)]	139.1	139.3	139.1
r[C(6)−C(1)]	140.2	139.3	138.9
r[C(1)−N(11)]	141.2	140.9	140.7
r[C(2)−S(14)]	177.6	182.6	181.6
r[N(13)−S(14)]	173.4	169.7	168.9
r[S(12)−N(13)]	160.3	156.5	155.7
r[N(11)−S(12)]	158.9	156.7	155.8
r[C(3)−F(7)]	134.4	135.3	135.9
r[C(4)−H(8)]	108.5	108.2	107.9
r[C(5)−F(9)]	134.6	134.8	134.5
r[C(6)−H(10)]	108.6	108.3	108.0
a[C(6)−C(1)−C(2)]	120.7	119.4	119.4
a[C(5)−C(6)−C(1)]	118.6	119.8	119.8
a[C(4)−C(5)−C(6)]	122.6	122.5	122.5
a[F(7)−C(3)−C(4)]	118.0	117.9	118.0
a[H(8)−C(4)−C(5)]	121.7	122.5	122.4
a[F(9)−C(5)−C(6)]	118.9	118.4	118.4
a[H(10)−C(6)−C(2)]	120.0	119.4	119.6
a[N(11)−C(1)−C(2)]	123.3	124.7	124.4
a[S(14)−N(13)−S(12)]	116.4	124.9	124.3
a[N(13)−S(14)−C(2)]	100.5	103.9	104.5
a[S(14)−C(2)−C(1)]	121.2	125.1	124.9
d[N(11)−C(1)−C(2)−S(14)]	12.8	0.0	0.0
d[S(12)−N(13)−S(14)−C(2)]	42.6	0.0	0.0
d[N(13)−S(14)−C(2)−C(1)]	−44.5	0.0	0.0
d[S(14)−C(2)−C(1)−C(6)]	−176.1	180.0	180.0

[a] Ref.[14] [b] Dunning correlation-consistent triple-ζ with diffuse functions.[16]

mates for the u_{h1} values. Table 5 lists the experimental frequencies as well as the scaled theoretical frequencies. The scaling factors for the theoretical frequencies were 0.92 for CH stretching modes, 0.98 for CH out-of-plane bending modes and 0.97 for the CC stretching modes. The RMS difference between the experimental and theoretical frequencies is 9 cm^{-1} and the largest difference is 17 cm^{-1}.

The refinement was carried out using the ed@ed program.[8] SARACEN restraints were applied to a large number of the independent parameters in order to allow all similar distances to be refined simultaneously. All the restraints are listed in Table 4. Reasonably tight restraints were applied to all the parameters describing the carbocyclic fragment since the consistency of the calculations gave us a large amount of confidence in the computed values for these parameters. Restraints were also placed on the C−H distance and C−F distance parameters (p_8 and p_9, respectively). The only restraints applied to the heterocyclic fragment were to the S−N distance average and difference parameters (p_{12} and p_{13}, respectively). The starting values for the refinement and the values for the restraints were taken from a DFT calculation using the B3LYP functional with a Dunning correlation-consistent basis set of triple-ζ quality, augmented by one diffuse function on each atom.[16]

It is immediately obvious that the positions of the hydrogen atoms are determined almost entirely by the restraints, with the exception of the C−H bond length. All of the difference parameters pertaining to the structure of the carbocycle (p_2−p_7) are also determined by the restraints (indicated by the equivalence of the parameter estimated standard deviation, e.s.d., and the restraint uncertainty). The unrestrained parameter p_1 (the average of the C−C and C−N distances) differs by just 0.5 pm from the computed value (DFT/B3LYP/aug-cc-pVTZ). The remaining restrained parameter values fall within the restraint uncertainties apart from p_{20}, the value of which lies just outside the uncertainty range of the restraint.

Restraints were also applied to the RMS amplitudes of vibration which could not be refined independently. Values for these restraints were calculated directly from the DFT force field, with uncertainties of 10% in the absolute computed values. With these restraints in place, all the significant RMS amplitudes of vibration were refined. The full set of refined RMS amplitudes of vibration is presented as Supporting Information (Table S1; for Supporting Informations see also the footnote on the first page of this article) along with their associated interatomic distances. The final R_G factor for the refinement was 0.049 (for the individual datasets: $R_G^{(long)} = 0.155$; $R_G^{(long)} = 0.032$). The molecu-

Table 3. Results of theoretical calculations for compound **4**; all distances in pm and all angles in degrees

Parameter	MP2 6-311+G*[a]	DFT-B3LYP 6-311+G*[a]	aug-cc-pVTZ[b]
r[C(1)−C(2)]	141.0	141.0	140.5
r[C(2)−C(3)]	139.6	138.3	137.9
r[C(3)−C(4)]	139.3	139.5	139.3
r[C(4)−C(5)]	139.4	138.2	137.8
r[C(5)−C(6)]	139.6	139.8	139.7
r[C(6)−C(1)]	140.5	139.7	139.4
r[C(1)−N(11)]	140.4	140.2	140.2
r[C(2)−S(14)]	177.7	181.4	180.9
r[N(13)−S(14)]	173.6	171.3	170.0
r[S(12)−N(13)]	160.0	156.8	156.0
r[N(11)−S(12)]	159.4	156.6	155.6
r[C(3)−H(7)]	108.7	108.5	108.1
r[C(4)−F(8)]	133.7	134.0	133.8
r[C(5)−F(9)]	133.2	133.5	133.3
r[C(6)−F(10)]	132.9	133.2	133.0
a[C(6)−C(1)−C(2)]	117.8	117.4	117.4
a[C(5)−C(6)−C(1)]	121.3	121.9	121.9
a[C(4)−C(5)−C(6)]	119.3	119.1	119.0
a[H(7)−C(3)−C(4)]	119.5	118.7	118.7
a[F(8)−C(4)−C(5)]	118.6	119.4	119.4
a[F(9)−C(5)−C(6)]	120.1	119.9	119.8
a[F(10)−C(6)−C(2)]	120.5	120.2	120.2
a[N(11)−C(1)−C(2)]	125.3	125.6	125.5
a[S(14)−N(13)−S(12)]	116.2	121.7	122.2
a[N(13)−S(14)−C(2)]	100.6	103.8	105.0
a[S(14)−C(2)−C(1)]	118.9	121.6	122.2
d[N(11)−C(1)−C(2)−S(14)]	15.4	8.2	6.0
d[S(12)−N(13)−S(14)−C(2)]	43.9	25.2	18.8
d[N(13)−S(14)−C(2)−C(1)]	−46.6	−26.1	−19.3
d[S(14)−C(2)−C(1)−C(6)]	−174.6	−176.0	−176.9

[a] Ref.[14] [b] Dunning correlation-consistent triple-ζ with diffuse functions.[16]

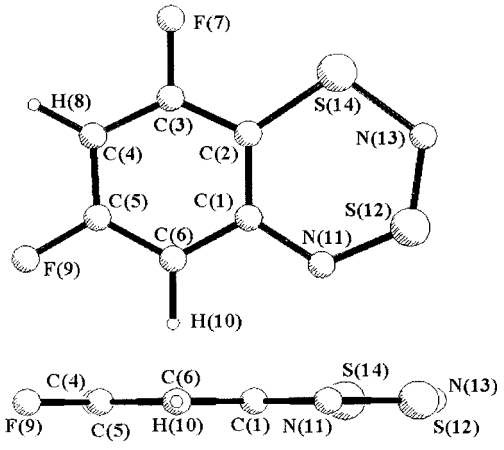

Figure 1. Refined molecular structure and atom numbering scheme for 6,8-difluoro-1,3λ⁴δ²,2,4-benzodithiadiazine (**3**)

lar scattering intensities are available in the Supporting Information (Figure S1) and the final RDCs are shown in Figure 2.

The parameters describing the folding of the heterocyclic ring ($p_{25}-p_{28}$), a key aspect of this study, were initially held fixed in the computed geometry (i.e. a planar conformation). Once this constrained refinement had been completed, the four folding parameters were combined into one parameter describing the folding motion (p_{25}), the other three parameters being determined from it by fixed ratios (as in Blockhuys et al.[3]). The ratios were determined from the displacements of the atoms of the heterocycle for the lowest-frequency folding mode calculated from the DFT force field [$p_{26} = 3.05 \times p_{25}$; $p_{27} = -3.46 \times p_{25}$; $p_{28} = (0.39 \times p_{25}) - 180$]. This folding parameter was then fixed at various nonzero values and the refinement repeated. The variation of the R_G factor with folding angle was monitored and is plotted in Figure 3. It is immediately obvious that the molecule adopts the planar conformation in the gas phase. The tables of Hamilton[17] were used to compute the 99.5% confidence limit (ca. 3σ) in order to determine the estimated standard deviation for the folding angle, leading to a value of 0.0(5)° (where the figure in parentheses indicates the e.s.d. in the last digit). The refined values of the structural parameters (r_{h1} structure) of this conformation are shown in Table 4. The planar conformation is in agreement with both the predictions of the π-fluoro hypothesis and those of the DFT calculations.

The Supporting Information (see also footnote on the first page of article) contains numerical data corresponding to the molecular scattering intensity curves (Table S2) and

Table 4. Independent and dependent geometrical parameters (r_{h1}) from the SARACEN GED structural refinement of compound **3**; figures in parentheses are the estimated standard deviations of the last digits; all distances in pm and all angles in degrees

	Parameter	GED	Restraint/constraint
Independent parameters			
p_1	av{*r*[C−C], *r*[C−N]}	140.0(2)	
p_2	av{*r*[C(1)−C(2)], *r*[C(3)−C(4)], *r*[C(1)−C(6)], *r*[C(1)−N(11)]} − av{*r*[C(2)−C(3)], *r*[C(4)−C(5)], *r*[C(5)−C(6)]}	2.0(1)	2.0(1)
p_3	*r*[C(5)−C(6)] − av{*r*[C(2)−C(3)], *r*[C(4)−C(5)]}	1.7(1)	1.7(1)
p_4	*r*[C(2)−C(3)] − *r*[C(4)−C(5)]	0.1(1)	0.1(1)
p_5	*r*[C(1)−C(2)] − av{*r*[C(3)−C(4)], *r*[C(1)−C(6)], *r*[C(1)−N(11)]}	1.2(1)	1.2(1)
p_6	*r*[C(1)−N(11)] − av{*r*[C(3)−C(4)], *r*[C(1)−C(6)]}	1.5(1)	1.5(1)
p_7	*r*[C(3)−C(4)] − *r*[C(1)−C(6)]	0.6(1)	0.6(1)
p_8	av{*r*[C−H]}	108.6(10)	107.9(10)
p_9	av{*r*[C−F]}	134.5(5)	134.6(10)
p_{10}	*r*[C(2)−S(14)]	176.6(8)	
p_{11}	*r*[S(14)−N(13)]	175.8(5)	
p_{12}	av{*r*[S(12)−N(13)], *r*[S(12)−N(11)]}	155.7(7)	155.8(10)
p_{13}	*r*[S(12)−N(13)] − *r*[S(12)−N(11)]	−0.1(1)	−0.1(1)
p_{14}	*a*[C(6)−C(1)−C(2)]	119.6(4)	119.4(5)
p_{15}	*a*[C(5)−C(6)−C(1)]	120.2(3)	119.8(5)
p_{16}	*a*[C(4)−C(5)−C(6)]	123.0(5)	122.5(5)
p_{17}	*a*[H(10)−C(6)−C(1)]	119.7(5)	119.6(5)
p_{18}	*a*[F(9)−C(5)−C(6)]	118.8(5)	118.4(5)
p_{19}	*a*[H(8)−C(4)−C(5)]	122.3(5)	122.4(5)
p_{20}	*a*[F(7)−C(3)−C(4)]	117.3(5)	118.0(5)
p_{21}	*a*[N(11)−C(1)−C(2)]	124.4(5)	
p_{22}	*a*[S(14)−N(13)−S(12)]	119.9(4)	
p_{23}	*a*[N(13)−S(14)−C(2)]	106.3(3)	
p_{24}	*a*[S(14)−C(1)−C(2)]	125.6(4)	
p_{25}	*d*[N(11)−C(1)−C(2)−S(14)]	0.0(5)	
p_{26}	*d*[S(12)−N(13)−S(14)−C(2)]	0.0	tied to p_{25}
p_{27}	*d*[N(13)−S(14)−C(2)−C(1)]	0.0	tied to p_{25}
p_{28}	*d*[S(14)−C(2)−C(1)−C(6)]	180.0	tied to p_{25}
Dependent parameters			
d_1	*r*[C(1)−C(2)]	141.8(2)	
d_2	*r*[C(2)−C(3)]	138.4(2)	
d_3	*r*[C(3)−C(4)]	140.4(2)	
d_4	*r*[C(4)−C(5)]	138.3(2)	
d_5	*r*[C(5)−C(6)]	140.0(2)	
d_6	*r*[C(1)−C(6)]	139.8(2)	
d_7	*r*[C(1)−N(11)]	141.6(2)	
d_8	*r*[N(11)−S(12)]	155.8(7)	
d_9	*r*[N(13)−S(12)]	155.7(7)	

the R_G factor plot (Table S3) along with the Cartesian coordinates of the final refined structure (Table S4) and the least-squares correlation matrix (Table S5).

5,6,7-Trifluoro-1,3λ⁴δ²,2,4-benzodithiadiazine (4)

The model for compound **4** was constructed in an analogous way to that for compound **3**. Figure 4 shows the refined structure and atom numbering scheme for compound **4**. The differences between the models are listed below:

p_8 now describes only one C−H bond length.

p_9 now describes three C−F distances.

p_{19} now describes an F−C−C angle.

IR and Raman spectra were recorded and used to scale the calculated force-field (computed in an analogous way to that for compound **3**) to obtain the most realistic estimates of the u_{h1} values. Table 6 lists the experimental frequencies as well as the scaled theoretical frequencies. The scaling factors for the theoretical frequencies were 0.92 for CH stretching modes, 0.98 for CH out-of-plane bending modes and 0.97 for the CC stretching modes. The RMS difference between the experimental and theoretical frequencies is 9 cm^{-1} and the largest difference is 17 cm^{-1}.

Once again, SARACEN restraints were applied to many of the independent parameters in order to allow all similar distances to be refined simultaneously. All the restraints are listed in Table 7. Restraints were also placed on the C−H distance and C−F distance parameters (p_8 and p_9, respectively). The only restraints applied to the heterocyclic fragment were on the S−N average distance parameter and the S−N distance difference parameter (p_{12} and p_{13}). The starting values for the refinement and the values for the restraints were taken from a DFT calculation using the B3LYP functional with a Dunning correlation-consistent basis set of triple-ζ quality augmented with one diffuse function on each atom.

Table 5. Experimental and scaled theoretical vibrational data for compound **3**; see text for scaling factors; frequencies ($\tilde{\nu}$) in cm^{-1}, IR intensities (I) in $km \cdot mol^{-1}$

$\tilde{\nu}_{calcd.}$	($I_{calcd.}$)	$\tilde{\nu}_{exp}$ [a]		$\tilde{\nu}_{calcd.}$	($I_{calcd.}$)	$\tilde{\nu}_{exp}$ [a]	
3102	(3)	3099	r	713	(7)		
3092	(1)	3081	r	617	(46)	629	m
1615	(102)	1632	w	609	(8)	615	m
1606	(116)	1595	m	603	(4)	602	m
1467	(114)	1460	m	592	(2)	581	vw
1422	(63)	1415	r	559	(3)	566	r
1353	(21)	1338	m	514	(11)	519	w
1280	(13)	1295	r	478	(13)	476	w
1195	(41)	1187	r	372	(0)	371	r
1139	(211)	1136	r	361	(1)		
1105	(21)	1106	w	359	(6)		
1044	(17)	1052	r	321	(5)		
1012	(56)	1017	m	293	(2)	299	r
1000	(13)	1000	m	241	(2)		
890	(19)	896	r	212	(1)		
873	(29)	860	m	201	(0)		
832	(21)	836	m	95	(0)		
724	(3)			21	(1)		

[a] vw: very weak; w: weak; m: medium; r: Raman band not observed in IR.

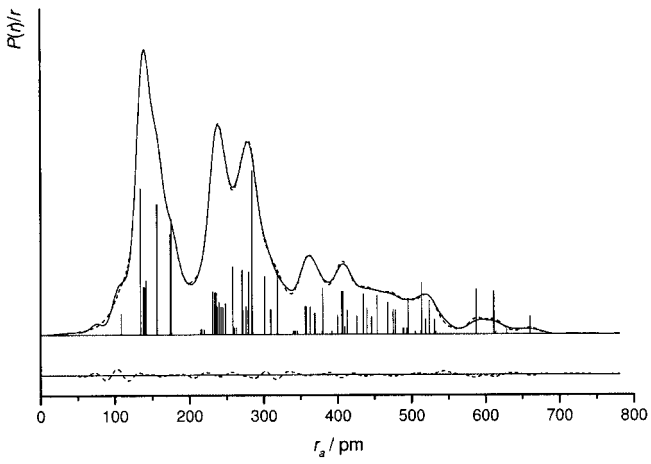

Figure 2. Radial distribution and difference curves for compound **3**; solid curve: observed radial distribution curve; dashed curve: calculated radial distribution curve at refined geometry; lower dashed curve: difference between observed and calculated radial distribution curves; before Fourier inversion all data were multiplied by $s[\exp(-0.00002s^2)/(Z_S - f_S)(Z_F - f_F)]$

Restraints were also applied to the RMS amplitudes of vibration which could not be refined independently. Values for these restraints were calculated directly from the DFT force field, with uncertainties of 10% in the absolute computed values. With these restraints in place, all the significant RMS amplitudes of vibration were refined. The full set of refined RMS amplitudes of vibration is available in the Supporting Information (Table S6) along with their associated interatomic distances. The final R_G factor for the refinement was 0.039 (for the individual data sets: $R_G^{(short)} = 0.112$; $R_G^{(long)} = 0.025$). The molecular scattering intensities are available in the Supporting Information (Figure S2) and the final RDCs are shown in Figure 5. Once again, all of

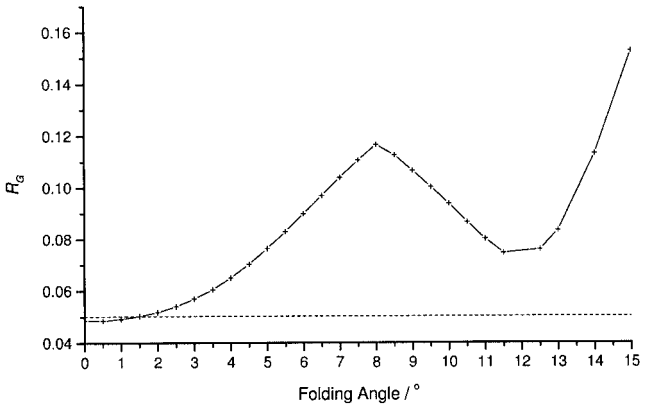

Figure 3. Variation of R_G with folding angle of the heterocyclic fragment for compound **3**; a 0° folding angle corresponds to the planar conformation; the dashed line marks the 99.5% confidence limit

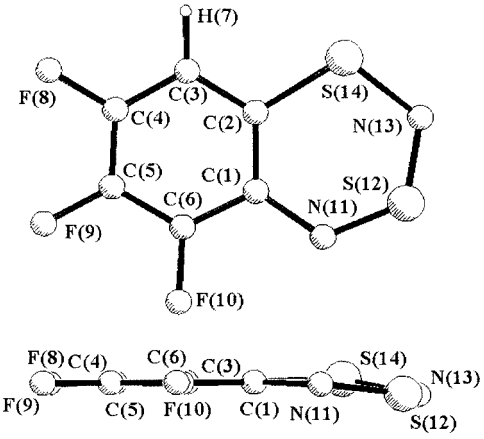

Figure 4. Refined molecular structure and atom numbering scheme for 5,6,7-trifluoro-1,3λ⁴δ²,2,4-benzodithiadiazine (**4**)

Table 6. Experimental and scaled theoretical vibrational data for compound **4**; see text for scaling factors; frequencies ($\tilde{\nu}$) in cm^{-1}, IR intensities (I) in $km \cdot mol^{-1}$

$\tilde{\nu}_{calcd.}$	($I_{calcd.}$)	$\tilde{\nu}_{exp}$ [a]		$\tilde{\nu}_{calcd.}$	($I_{calcd.}$)	$\tilde{\nu}_{exp}$ [a]	
3054	(2)	3048	w	655	(1)		
1625	(66)	1614	m	616	(33)	631	m
1604	(20)	1595	m	569	(4)	561	w
1501	(342)	1505	s	535	(3)	541	w
1443	(147)	1439	s	511	(5)	519	w
1352	(35)	1340	m	458	(7)	449	w
1276	(46)	1274	w	414	(1)	421	w
1257	(6)	1244	m	359	(7)		
1218	(66)	1215	m	340	(1)		
1119	(140)	1136	s	327	(6)		
1059	(82)	1068	s	294	(5)		
995	(27)	1007	m	281	(2)		
924	(4)	930	w	275	(1)		
860	(18)	858	m	220	(0)		
811	(35)	821	m	178	(1)		
757	(6)	743	m	148	(0)		
742	(10)			100	(0)		
677	(21)	678	m	51	(0)		

[a] w: weak; m: medium; s: strong.

Table 7. Independent and dependent geometrical parameters (r_{h1}) from the SARACEN GED structural refinement of compound **4**; figures in parentheses are the estimated standard deviations of the last digits; all distances in pm and all angles in degrees

	Parameter	GED	Restraint/constraint
Independent parameters			
p_1	av{*r*[C−C], *r*[C−N]}	139.9(2)	
p_2	av{*r*[C(1)−C(2)], *r*[C(3)−C(4)], *r*[C(1)−C(6)], *r*[C(1)−N(11)]} − av{*r*[C(2)−C(3)], *r*[C(4)−C(5)], *r*[C(5)−C(6)]}	1.3(5)	1.4(5)
p_3	*r*[C(5)−C(6)] − av{*r*[C(2)−C(3)], *r*[C(4)−C(5)]}	1.6(5)	1.6(5)
p_4	*r*[C(2)−C(3)] − *r*[C(4)−C(5)]	0.1(1)	0.1(1)
p_5	*r*[C(1)−C(2)] − av{*r*[C(3)−C(4)], *r*[C(1)−C(6)], *r*[C(1)−N(11)]}	1.1(5)	1.2(5)
p_6	*r*[C(1)−N(11)] − av{*r*[C(3)−C(4)], *r*[C(1)−C(6)]}	0.6(1)	0.6(1)
p_7	*r*[C(3)−C(4)] − *r*[C(1)−C(6)]	−0.2(1)	−0.2(1)
p_8	*r*[C−H]	108.2(10)	108.94(10)
p_9	av{*r*[C−F]}	133.5(4)	133.6(5)
p_{10}	*r*[C(2)−S(14)]	180.6(8)	
p_{11}	*r*[S(14)−N(13)]	170.7(6)	
p_{12}	av{*r*[S(12)−N(13)], *r*[S(12)−N(11)]}	155.5(7)	155.6(10)
p_{13}	*r*[S(12)−N(13)] − *r*[S(12)−N(11)]	0.2(1)	0.3(1)
p_{14}	*a*[C(6)−C(1)−C(2)]	116.9(6)	
p_{15}	*a*[C(5)−C(6)−C(1)]	121.8(7)	
p_{16}	*a*[C(4)−C(5)−C(6)]	118.7(6)	
p_{17}	*a*[H(7)−C(6)−C(1)]	119.9(5)	120.2(10)
p_{18}	*a*[F(8)−C(5)−C(6)]	119.4(7)	119.8(10)
p_{19}	*a*[F(9)−C(4)−C(5)]	119.7(7)	119.4(10)
p_{20}	*a*[F(10)−C(3)−C(4)]	118.6(10)	118.7(10)
p_{21}	*a*[N(11)−C(1)−C(2)]	125.7(8)	
p_{22}	*a*[S(14)−N(13)−S(12)]	119.9(8)	
p_{23}	*a*[N(13)−S(14)−C(2)]	106.9(6)	
p_{24}	*a*[S(14)−C(1)−C(2)]	122.6(6)	
p_{25}	*d*[N(11)−C(1)−C(2)−S(14)]	4.0(−30;+3)	
p_{26}	*d*[S(12)−N(13)−S(14)−C(2)]	12.2	tied to p_{25}
p_{27}	*d*[N(13)−S(14)−C(2)−C(1)]	−12.6	tied to p_{25}
p_{28}	*d*[S(14)−C(2)−C(1)−C(6)]	−178.0	tied to p_{25}
Dependent parameters			
d_1	*r*[C(1)−C(2)]	141.3(5)	
d_2	*r*[C(2)−C(3)]	138.6(4)	
d_3	*r*[C(3)−C(4)]	139.9(3)	
d_4	*r*[C(4)−C(5)]	138.5(4)	
d_5	*r*[C(5)−C(6)]	140.2(4)	
d_6	*r*[C(1)−C(6)]	140.1(3)	
d_7	*r*[C(1)−N(11)]	140.6(2)	
d_8	*r*[N(11)−S(12)]	154.6(7)	
d_9	*r*[N(13)−S(12)]	155.6(7)	

the difference parameters defining the structure of the carbocycle (p_2−p_7) are determined entirely by the restraints. The unrestrained parameter describing the average of the C−C and C−N distances (p_1) differs by just 0.3 pm from the computed value (DFT/B3LYP/aug-cc-pVTZ).

As for compound **3**, we were particularly interested in the planarity or nonplanarity of the heterocyclic fragment. In order to investigate this, the four parameters describing the folding of the heterocyclic fragment were combined into just one folding parameter (p_{25}). The ratios were determined from the displacements of the atoms of the heterocycle for the lowest-frequency folding mode calculated from the DFT force field [$p_{26} = 3.05 \times p_{25}$; $p_{27} = -3.16 \times p_{25}$; $p_{28} = (0.49 \times p_{25}) - 180$]. This parameter was fixed at various values and the refinement repeated. The variation of the R_G factor with folding angle is presented in Figure 6 along with the 99.5% confidence limit, calculated as described above. The graph indicates that the folding angle parameter can take effectively any value between 0° (planar) and about 6°. The variation of the R_G factor from its minimum value of 0.038 (4.0°) up to its value of 0.042 at 6° is just 0.004. Nevertheless, the R_G factor analysis suggests a folding angle of 4.0(−30;+3)°. More evidence for the slightly nonplanar geometry of the heterocyclic fragment comes from the fact that in the refinement at the planar geometry, some of the parameter values lie outside their SARACEN restraint uncertainties. In the nonplanar geometry refinement the parameter values lie within the restraint uncertainties.

The Supporting Information contains numerical data corresponding to the molecular scattering intensity curves (Table S7) and the R_G factor plot (Table S8) along with the Cartesian coordinates of the final refined structure (Table S9) and the least-squares correlation matrix (Table S10).

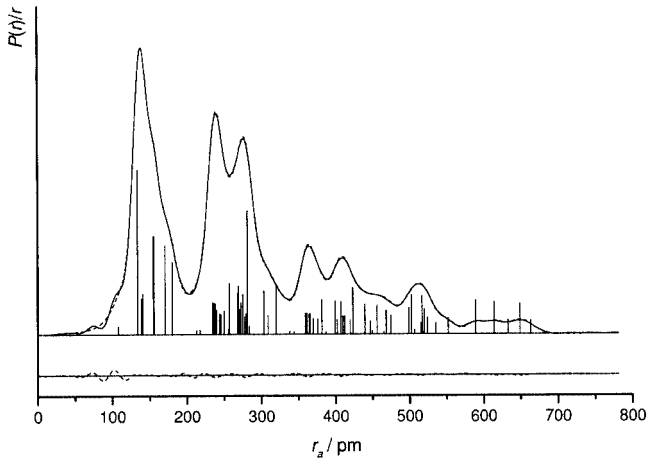

Figure 5. Radial distribution and difference curves for compound **4**; solid curve: observed radial distribution curve; dashed curve: calculated radial distribution curve at refined geometry; lower dashed curve: difference between observed and calculated radial distribution curves; before Fourier inversion all data were multiplied by $s[\exp(-0.00002s^2)/(Z_S - f_S)(Z_F - f_F)]$

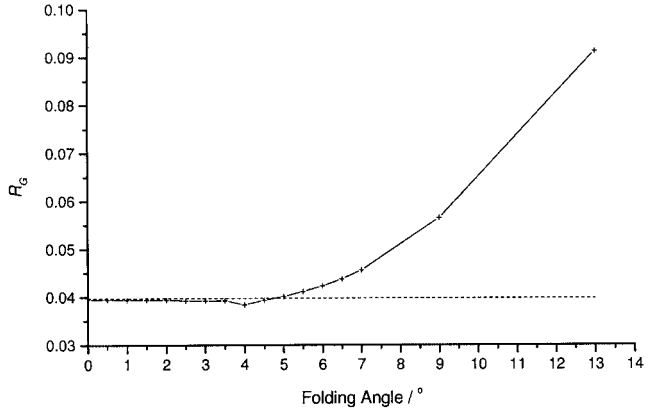

Figure 6. Variation of R_G with folding angle of the heterocyclic fragment for compound **4**; a 0° folding angle corresponds to the planar conformation; the dashed line marks the 99.5% confidence limit

Structural Comparisons

Table 8 enables a comparison of the available experimental and theoretical structural data (DFT/B3LYP/aug-cc-pVTZ) for compound **3** and Table 9 shows the same comparison for compound **4**.

For compound **3**, both GED and theory agree on a planar conformation with respect to the heterocyclic ring in the gas phase, while the XRD study shows that the compound is bent in the crystal. The major differences between the GED structure and the theoretical structure are in the S(14)−N(13) and C(1)−S(14) bond lengths. In the GED structure, the S(14)−N(13) bond is 6.9 pm longer than the theoretical value and the C(2)−S(14) bond length is 5 pm shorter than the theoretical value. Refinements with the bond lengths restrained to the theoretical distances show significantly larger R_G factors than for the final refined structure. 1st row to 2nd row *p*-block bond lengths have been found to be particularly difficult to determine using ab initio techniques.[18]

Table 8. Comparison of pertinent structural parameters from different techniques for compound **3**; all distances in pm and all angles in degrees

Parameter	GED (r_{h1})[a]	XRD[b]	Theory (r_e)[a]
r[S(14)−N(13)]	175.8(5)	166.8(5)	168.9
r[N(13)−S(12)]	155.7(7)	155.1(5)	155.7
r[S(12)−N(11)]	155.8(7)	153.6(5)	155.8
r[N(11)−C(1)]	141.6(2)	142.5(6)	140.7
r[C(1)−C(2)]	141.8(2)	139.8(7)	140.9
r[C(2)−S(14)]	176.6(8)	177.9(5)	181.6
a[S(14)−N(13)−S(12)]	119.9(4)	123.9(3)	124.3
a[N(13)−S(12)−N(11)]	121.6(4)	118.3(2)	118.8
a[S(12)−N(11)−C(1)]	122.2(4)	123.2(4)	123.1
a[N(11)−C(1)−C(2)]	124.4(5)	123.6(4)	124.4
a[C(1)−C(2)−S(14)]	125.6(4)	124.6(4)	124.9
a[C(2)−S(14)−N(13)]	106.3(3)	105.0(2)	104.5
d[N(11)−C(1)−C(2)−S14)]	0.0(5)	8.2(8)	0.0

[a] This work (DFT/B3LYP/aug-cc-pVTZ). [b] Makarov et al.[4]

Table 9. Comparison of pertinent structural parameters from different techniques for compound **4**; all distances in pm and all angles in degrees

Parameter	GED (r_{h1})[a]	XRD[b]	Theory (r_e)[a]
r[S(14)−N(13)]	170.7(6)	168.3(5)	170.0
r[N(13)−S(12)]	155.6(7)	153.9(5)	156.0
r[S(12)−N(11)]	154.6(7)	153.2(4)	155.6
r[N(11)−C(1)]	140.6(3)	143.0(6)	140.2
r[C(1)−C(2)]	141.3(5)	138.9(7)	140.5
r[C(2)−S(14)]	180.6(8)	178.6(5)	180.9
a[S(14)−N(13)−S(12)]	119.9(8)	123.9(3)	122.2
a[N(13)−S(12)−N(11)]	121.8(6)	119.7(2)	118.5
a[S(12)−N(11)−C(1)]	121.6(6)	121.4(4)	122.5
a[N(11)−C(1)−C(2)]	125.8(8)	125.7(4)	125.5
a[C(1)−C(2)−S(14)]	122.6(6)	123.9(4)	122.2
a[C(2)−S(14)−N(13)]	106.9(6)	105.3(2)	105.0
d[N(11)−C(1)−C(2)−S(14)]	4.0(−30;+3)	1.7(7)	6.0

[a] This work (DFT/B3LYP/aug-cc-pVTZ). [b] Makarov et al.[4]

For compound **4**, the theoretical structure shows a bent conformation for the heterocyclic ring and the XRD study shows that the heterocycle is almost flat in the crystal. In the gas phase, the indications are that the heterocyclic ring is slightly bent. This is supported by the fact that generally, the GED structural parameters agree more closely with the theoretical (bent) structure than with the XRD (almost planar) structure. All the S−N bond lengths and the C−S bond length agree to within 1 pm. The magnitude of the folding angle is also very similar in the GED and theoretical structures.

Table 10 shows a comparison of the relevant structural parameters for compounds **1**, **2**, **3** and **4** as determined by GED. The major differences between the compounds are in the S(14)−N(13) and C(2)−S(14) bond lengths. For the S(14)−N(13) bond, the largest difference is 6.1 pm (between compound **1** and compound **3**) and for the C(2)−S(14) bond length, the largest difference is 4.6 pm (between compound **2** and compound **3**). It is worth noting that although the S=N bond lengths [N(11)−S(12), S(12)−N(13)] stay

Table 10. Comparison of pertinent structural parameters (r_{h1}) from GED structural refinements of benzodithiadiazine derivatives; all distances in pm and all angles in degrees

Parameter	Compound 1[a]	2[a]	3[b]	4[b]
r[S(14)−N(13)]	169.7(5)	172.3(8)	175.8(5)	170.7(6)
r[N(13)−S(12)]	154.8(3)	155.3(3)	155.7(7)	155.6(7)
r[S(12)−N(11)]	154.3(3)	155.2(3)	155.8(7)	154.6(7)
r[N(11)−C(1)]	139.3(6)	139.6(7)	141.6(2)	140.6(3)
r[C(1)−C(2)]	139.1(6)	140.5(8)	141.8(2)	141.3(5)
r[C(2)−S(14)]	178.4(5)	181.2(9)	176.6(8)	180.6(8)
a[S(14)−N(13)−S(12)]	119.9(5)	122.8(5)	119.9(4)	119.9(8)
a[N(13)−S(12)−N(11)]	−	−	121.6(4)	121.8(6)
a[S(12)−N(11)−C(1)]	−	−	122.2(4)	121.6(6)
a[N(11)−C(1)−C(2)]	123.3(7)	125.4(7)	124.4(5)	125.8(8)
a[C(1)−C(2)−S(14)]	122.7(6)	124.6(6)	125.6(4)	122.6(6)
a[C(2)−S(14)−N(13)]	101.5(7)	104.5(3)	106.3(3)	106.9(6)
d[N(11)−C(1)−C(2)−S(14)]	−17.0(30)	0.0(5)	0.0(5)	4.0(−30;+3)

[a] Blockhuys et al.[3] [b] This work.

reasonably consistent over all the compounds, the S−N bond length [S(14)−N(13)] is slightly greater in the two planar compounds. The lack of other obvious trends in the structures is indicative of the complex effects that different fluorine substitution patterns have on the structures of the compounds. Although the calculations predict that both the S(14)−N(13) and C(2)−S(14) bond lengths should be similar in both compounds **3** and **4**, the GED results do not replicate this trend. To assess whether or not this is a real effect we restrained the values in the GED refinement to the theoretical values. In both compounds this resulted in the values lying well outside the restraint uncertainties and a large increase in the R_G factors showing that the experimentally determined values are indeed correct.

Our studies show that compound **3** is planar and that compound **4** is slightly nonplanar, in line with the π-fluoro hypothesis. The energy difference between the planar and nonplanar conformations of compound **4** has been calculated using a number of different methods and the results are shown in Table 11. These values have been corrected by adding the calculated zero-point vibrational energies (scaled according to the constants of Wong et al.). All of the energy differences between the bent and flat conformers are effectively zero, reflecting the low-frequency, large-amplitude nature of the out-of-plane bending mode. At the temperature of the GED experiment we would expect the vibrational mode corresponding to the folding of the heterocyclic ring to have a large amplitude, leading to the very large uncertainties we see in the value of the folding angle.

Table 11. Calculated energy differences between bent and flat conformations of compound **4**; all energy differences include scaled zero-point vibrational energy corrections

Method	Energy difference [kJ·mol^{-1}]
RHF/aug-cc-pVDZ	1.3
MP2/aug-cc-pVDZ	0.3
DFT/B3LYP/aug-cc-pVDZ	0.9
DFT/B3LYP/aug-cc-pVTZ	0.07

Conclusion

We have successfully used the new graphical structural refinement program ed@ed to obtain the SARACEN gas-phase structures of 6,8-difluoro-1,3λ^{4}δ^2,2,4-benzodithiadiazine (**3**) and 5,6,7-trifluoro-1,3λ^{4}δ^2,2,4-benzodithiadiazine (**4**) from GED data.

These GED structures have been compared with both the theoretical and crystal structures and the differences, in particular the conformations of the heterocyclic fragments, have been noted and discussed. Compound **3** is planar in the gas phase with respect to the heterocyclic fragment and compound **4** is slightly nonplanar, as predicted by the π-fluoro hypothesis postulated by Blockhuys et al.[3] The large uncertainties in the folding of the heterocyclic fragment for compound **4** are due to the low-frequency bending mode of the heterocyclic fragment. On the whole, this work and Blockhuys et al.[3] describe and explain interesting stereoelectronic effects in benzo-fused sulfur-nitrogen antiaromatic heterocycles. In particular, it has been shown that for free molecules, the conformation of the heterocyclic ring can be affected by substitutions on the carbocyclic fragment.

Acknowledgments

F. B. and C. V. A. gratefully acknowledge support from the University of Antwerp under Grant GOA-BOF-UA No. 23. We thank the UK Engineering and Physical Sciences Research Council for support for gas-phase electron diffraction (grant GR/R17768).

[1] A. V. Zibarev, Y. V. Gatilov, A. O. Miller, *Polyhedron* **1992**, *11*, 1137.
[2] A. W. Cordes, M. Hojo, H. Koenig, M. C. Noble, R. T. Oakley, W. T. Pennington, *Inorg. Chem.* **1986**, *25*, 1137.
[3] F. Blockhuys, S. L. Hinchley, A. Yu. Makarov, Y. V. Gatilov,

A. V. Zibarev, J. D. Woollins, D. W. H. Rankin, *Chem. Eur. J.* **2001**, *7*, 3592.

[4] A. Yu. Makarov, I. Yu. Bagryanskaya, F. Blockhuys, C. Van Alsenoy, Y. V. Gatilov, V. V. Knyazev, A. M. Maksimov, T. V. Mikhalina, V. E. Platonov, M. M. Shakirov, A. V. Zibarev, *Eur. J. Inorg. Chem.* **2003**, 77.

[5] P. V. Schastnev, L. N. Schegoleva, *Molecular Distortion in Ionic and Excited States*, CRC, Boca Raton, **1995**.

[6] C. M. Huntley, G. S. Laurenson, D. W. H. Rankin, *J. Chem. Soc., Dalton Trans.* **1980**, 954.

[7] Y. Murata, Y. Morino, *Acta Crystallogr.* **1966**, *20*, 605.

[8] S. L. Hinchley, H. E. Robertson, K. B. Borisenko, A. R. Turner, B. F. Johnston, D. W. H. Rankin, M. Ahmadian, J. N. Jones, A. H. Cowley, *Dalton Trans.*, in press.

[9] A. W. Ross, M. Fink, R. Hilderbrandt, in *International Tables for Crystallography* (Ed.: A. J. C. Wilson) Kluwer, Dordrecht, **1992**, vol. C, p. 245.

[10] M. J. Frisch, G. W. Trucks, H. B. Schlegel, G. E. Scuseria, M. A. Robb, J. R. Cheeseman, V. G. Zakrzewski, J. A. Montgomery, R. E. Stratmann, J. C. Burant, S. Dapprich, J. M. Millam, A. D. Daniels, K. N. Kudin, M. C. Strain, O. Farkas, J. Tomasi, V. Barone, M. Cossi, R. Cammi, B. Mennucci, C. Pomelli, C. Adamo, S. Clifford, J. Ochterski, G. A. Petersson, P. Y. Ayala, Q. Cui, K. Morokuma, D. K. Malick, A. D. Rabuck, K. Raghavachari, J. B. Foresman, J. Cioslowski, J. V. Ortiz, B. B. Stefanov, G. Liu, A. Liashenko, P. Piskorz, I. Komaromi, R. Gomperts, R. L. Martin, D. J. Fox, T. Keith, M. A. Al-Laham, C. Y. Peng, A. Nanayakkara, C. Gonzalez, M. Challacombe, P. M. W. Gill, B. G. Johnson, W. Chen, M. W. Wong, J. L. Andres, M. Head-Gordon, E. S. Replogle, J. A. Pople, *Gaussian98*, revision A.7, Gaussian Inc., Pittsburgh PA, **1998**.

[11] [11a] N. W. Mitzel, D. W. H. Rankin, *Dalton Trans.* **2003**, *19*, 3650. [11b] N. W. Mitzel, B. A. Smart, A. J. Blake, H. E. Robertson, D. W. H. Rankin, *J. Phys. Chem.* **1996**, *100*, 9339. [11c] A. J. Blake, P. T. Brain, H. McNab, J. Millar, C. A. Morrison, S. Parsons, D. W. H. Rankin, H. E. Robertson, B. A. Smart, *J. Phys. Chem.* **1996**, *100*, 12280.

[12] [12a] C. Møller, M. S. Plesset, *Phys. Rev.* **1934**, *46*, 618. [12b] M. Head-Gordon, J. A. Pople, M. J. Frisch, *Chem. Phys. Lett.* **1988**, *153*, 503. [12c] M. J. Frisch, M. Head-Gordon, J. A. Pople, *Chem. Phys. Lett.* **1990**, *166*, 275. [12d] M. J. Frisch, M. Head-Gordon, J. A. Pople, *Chem. Phys. Lett.* **1990**, *166*, 281. [12e] M. Head-Gordon, T. Head-Gordon, *Chem. Phys. Lett.* **1994**, *220*, 122. [12f] S. Saebo, J. Almlöf, *Chem. Phys. Lett.* **1989**, *154*, 83.

[13] [13a] A. D. Becke, *J. Chem. Phys.* **1993**, *98*, 5648; C. Lee, W. Yang, R. G. Parr, *Phys. Rev. B.* **1988**, *37*, 785. [13b] B. Miehlich, A. Savin, H. Still, H. Preuss, *Chem. Phys. Lett.* **1989**, *157*, 200.

[14] [14a] A. D. McLean, G. S. Chandler, *J. Chem. Phys.* **1980**, *72*, 5639. [14b] R. Krishnan, J. S. Binkley, R. Seeger, J. A. Pople, *J. Chem. Phys.* **1980**, *72*, 650. [14c] T. Clark, J. Chandrasekhar, G. W. Spitznagel, P. v. R. Schleyer, *J. Comp. Chem.* **1983**, *4*, 294.

[15] V. A. Sipachev, *J. Mol. Struct.* **1985**, *121*, 143; V. A. Sipachev, in *Advances in Molecular Structure Research* (Eds.: I. Hargittai, M. Hargittai), JAI, Greenwich, **1999**, vol. 5, p. 263.

[16] R. A. Kendall, T. H. Dunning Jr., R. J. Harrison, *J. Chem. Phys.* **1992**, *96*, 6796.

[17] W. C. Hamilton, *Acta Crystallogr.* **1965**, *18*, 502.

[18] S. L. Hinchley, P. Trickey, H. E. Robertson, B. A. Smart, D. W. H. Rankin, D. Leusser, B. Walfort, D. Stalke, M. Bühl, S. J. Obrey, *Dalton Trans.* **2002**, 4607.

Received July 12, 2004
Early View Article
Published Online December 6, 2004

